Accelerometer vs. Geophone Response: A Field Case History

Michael Hons*
University of Calgary, Calgary, AB
msjhons@ucalgary.ca

Robert Stewart, Don Lawton and Malcolm Bertram
University of Calgary, Calgary, AB, Canada

and

Glenn Hauer
ARAM Systems Ltd, Calgary, AB, Canada

Summary

A method is derived for the calculation of ground acceleration from geophone data using a frequency-domain inverse filter and an empirical scaling constant. Acceleration-domain spectra from geophones and MEMS accelerometers from an oilfield survey at Violet Grove, Alberta, Canada are compared. We find that the geophone and accelerometer data, over a band of 5-200 Hz, are very similar. The accelerometer amplitudes are larger than the geophones' below 5 Hz and there are some differences at very high frequencies. Significant events related to the first breaks are not observed on the accelerometer records at some stations.

Introduction

There has been considerable interest in the geophysical community surrounding the use of MEMS accelerometers as a new sensor in the acquisition of seismic data (Dragoset and Gabitzsch, 2007; Laine and Mougenot, 2007). It has been suggested that accelerometers, with their flat response in acceleration, may have advantages over geophones at low frequencies as well as high frequencies - due to greater sensitivity (Maxwell et al., 2001; Mougenot and Thorburn, 2004). If both sensors' frequency responses correspond to what the simple harmonic oscillator model would predict, then it should be straightforward to calculate an equivalent output in any domain desired. The output of the sensors could then be compared to show if differences are in evidence and whether either sensor more accurately represents ground motion.

Theory

Geophones and accelerometers are considered here as simple harmonic oscillators. This consists of a proof mass suspended from a damped spring. The motion of the proof mass in reference to the ground and sensor case is recorded as signal. The MEMS accelerometer is also controlled by a digital feedback system to prevent the proof mass from moving very far from a central reference position. At frequencies where the digital nature of the feedback can be ignored, the feedback

operates as another restoring force like a supplemental spring. This effectively very stiff spring, with its correspondingly high resonant frequency, means that the residual proof mass displacement detected in a MEMS accelerometer is directly proportional to the ground acceleration.

For a geophone, the velocity of the proof mass relative to the acceleration of the ground can be found from the simple harmonic oscillator equation and used to determine the ground acceleration from the geophone data. Taking the Fourier transform of the simple harmonic oscillator equation allows us to replace time derivatives with iω. Rearranging, as required for a geophone, gives

$$V_G = k_G \frac{\partial X}{\partial t} = k_G \frac{-i\omega}{-\omega^2 + 2i\lambda\omega\omega_0 + \omega_0^2} \frac{\partial^2 U}{\partial t^2},$$

where V_G is the voltage output from the geophone, k_G is the sensitivity (in V•s/m), X is the displacement of the proof mass, U is the displacement of the ground, ω_0 is the resonant frequency and λ is the damping factor.

The amplitude and phase response are shown in Figure 1a. The result relating to ground velocity is found by replacing one ∂/∂t on the right hand side with iω. The result relative to ground velocity is often referred to as the 'geophone equation', and has historically been of use because it shows that correcting the phase of the geophone-acquired data to zero gives a high-pass version of ground velocity (Figure 1b). There is no physical reason, however, that a geophone may represent only ground velocity and not ground acceleration or ground displacement.

Once we have acquired the geophone data, inverse filtering with

$$\frac{\partial^2 U}{\partial t^2} = \frac{1}{k_G} \frac{2\lambda\omega\omega_0 - i(\omega_0^2 - \omega^2)}{\omega} V_G,$$

gives ground acceleration amplitudes from geophone data. This data can then be directly compared to MEMS accelerometer data.

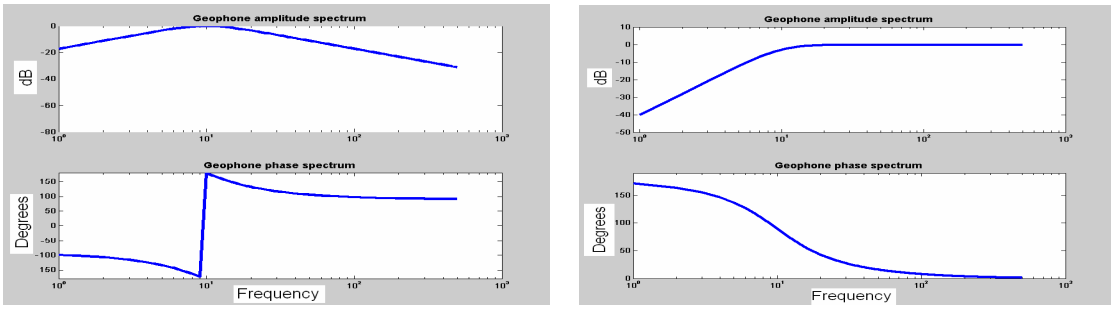

Figure1: a) Left: geophone response to ground acceleration. b) Right: geophone response to ground velocity.

Examples

Multicomponent seismic data were acquired in December, 2005 near Violet Grove, Alberta, Canada in the Pembina oil field. Three sensors (two 3C geophones and one Sercel DSU3-408 MEMS) were simultaneously laid out at 8 stations, with a separation of ~1 m from each other and a 20 m group spacing. At two stations, a third analog geophone was also planted (Figure 2a). Only the vertical component of the sensors is considered here. The geophones were recorded with an ARAM Aries instrument, while the accelerometers were connected to a Sercel 408UL system. The ground was solidly frozen when the sensors were laid out (Figure 2b), and warm water was used to

soften the earth so the sensors could be planted. The sensors then froze into the earth after planting, so in all cases coupling was excellent. A total of 222 dynamite shots were recorded. This provides a test case to observe differences between geophone and MEMS sensors.

Ground acceleration receiver gathers were calculated from each geophone, using its quoted sensitivity (with damping). These were compared to the DSU, assuming the DSU amplitudes represented mm/s^2. The DSU spectrum was very similar to those of the geophones, especially below the dominant peak down to ~5 Hz, but offset by a constant. Multiplying the DSU data by 1.25 gives the result in Figure 3a. The other receiver gathers were inspected to see if there was any appreciable deviation from this scaling factor at other stations or with varying amplitude, and none was observed (Figure 4a).

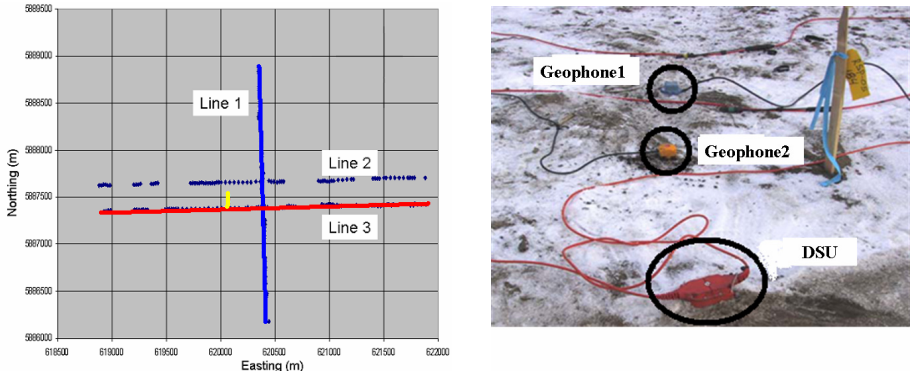

Figure 2: a) Left: Map of sensor test (blue-shots 1-75, red-shots150-222, yellow-receivers). b) Right: Sensors at a station (third geophone not present at this station)

Clearly some differences exists at high frequencies at station 5183 (Figure 3a). Comparison of results for shots 1-75 and shots 150-222 at stations 5183 and 5184 (Figures 3a and b, 4a and b), shows that the pattern of the spectra is consistent with station, but not consistent overall. At station 5183, the DSU recorded lower amplitudes just above the dominant frequency, and at frequencies above 100 Hz. At station 5184, this pattern was not evident. Close examination of station 5183 found that differences were largely constrained to the first breaks, especially those nearer the shot point. Figure 5 shows a time domain comparison where high frequency events following the large break are apparent in the geophone gather, but not in the DSU gather. Note that these are acceleration traces, so double integrating such high frequency events, even at large acceleration amplitudes, will mean those events were extremely small displacements. Apparently at some of the locations, conditions prevented the DSU from recording these very small high frequency events.

The amplitude spectra above will all be weighted toward the highest amplitudes, i.e. the early arrivals at near offsets. Comparison of amplitude spectra from gathers excluding these areas (Figure 6a), finds that the recorded amplitudes are very similar (Figure 6b). Even isolation of the smallest amplitudes (at late times, far offsets and before first breaks) failed to yield significant differences among the sensors between 5 and 200 Hz. It appears that over the data band that would most likely be included in, say, a deconvolution design window, the amplitude spectra acquired through the digital accelerometer and the analog geophone are quite similar.

At frequencies below 5 Hz, the DSU displays consistently higher amplitudes than the geophone. Whether the accelerometer is recording more signal or is noisier in this range is under investigation.

Conclusions

Generally, the two types of sensors appear to both record ground motion similarly. If data from the two sensor types must be merged, a scaling factor based on matching amplitude spectra should be found. The spectra should be broadly similar once the appropriate scaling is found, especially around the dominant frequency. We do observe some differences in the data related to high frequencies, very low frequencies, and near the first breaks.

Acknowledgements

Thanks to the CREWES sponsors for their support of research in advanced seismic methods.

References

Dragoset, B. and Gabitzsch, J. [2007] Introduction to this special section: Low-frequency seismic. The Leading Edge, **26**(1), 34-35.

Laine, J. and Mougenot, D. [2007] Benefits of MEMS based seismic accelerometers for oil exploration. Solid-state Sensors, Acuators and Microsystems Conference, 2007 (Transducers 2007), 1473-1477.

Maxwell, P., Tessman, J. and Reichert, B. [2001] Design through to production of a MEMS digital accelerometer for seismic acquisition. First Break, **19**(3), 141-144.

Mougenot, D. and Thorburn, N. [2004] MEMS-based 3C accelerometers for land seismic acquisition: Is it time? The Leading Edge, **23**(3), 246-250.

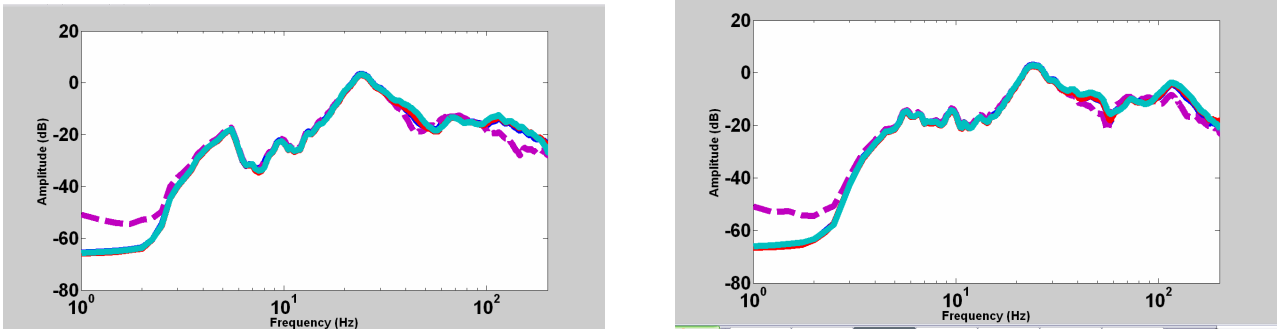

Figure 3: Amplitude spectra of four sensors at station 5183, empirical scaling. Amplitudes are dB-m/s^2, frequencies are 1-200 Hz. Solid lines (blue, red and cyan): geophones. Dashed line (purple): DSU. a) shots 1-75. b) shots 150-222.

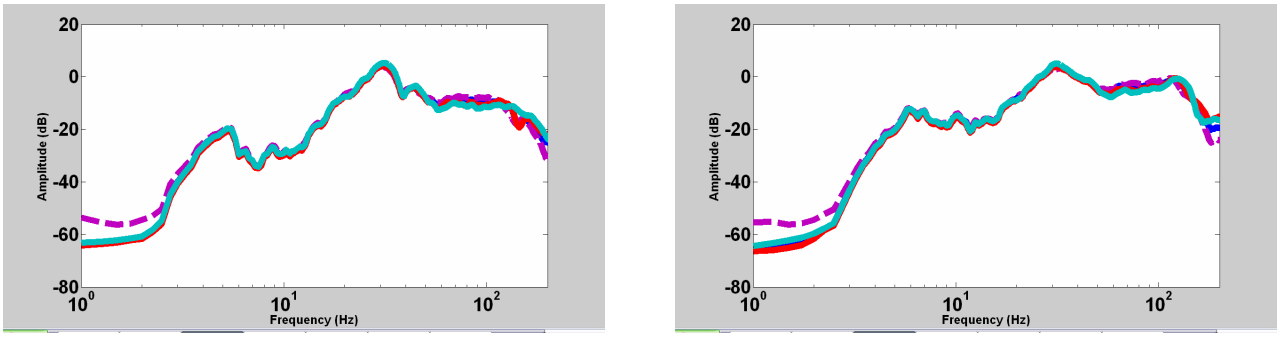

Figure 4: Amplitude spectra of four sensors at station 5184, empirical scaling. a) shots 1-75. b) shots 150-222

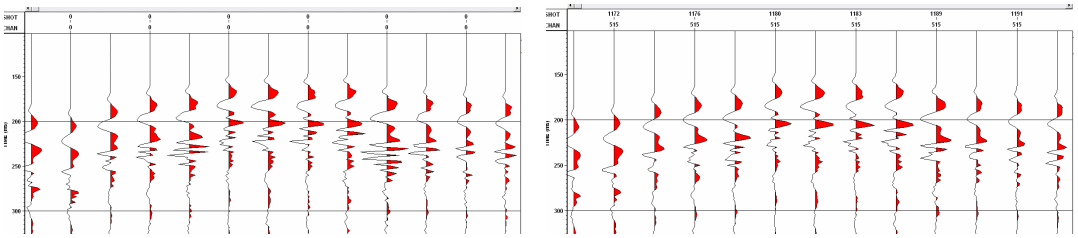

Figure 5: Left: Geophone1 gather, station 5183, shots 1-75. First breaks followed by high frequency events. Right: DSU gather, station 5183, shots 1-75. High frequency events absent.

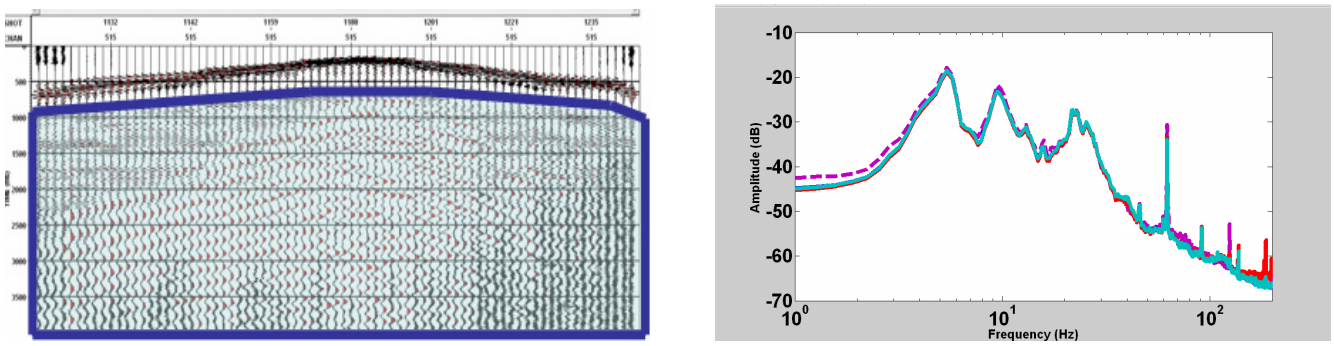

Figure 6: DSU receiver gather, station 5183, shots 1-75. Shaded blue is region that contributes to spectrum at right.